1-25-2018

Prediction of novel stable Fe-V-Si ternary phase

Manh Cuong Nguyen
Iowa State University and Ames Laboratory, mcnguyen@ameslab.gov

Chong Chen
Iowa State University and Ames Laboratory

Xin Zhao
Iowa State University and Ames Laboratory, xzhao@iastate.edu

Cai-Zhuang Wang
Iowa State University and Ames Laboratory, wangcz@ameslab.gov

Kai-Ming Ho
Iowa State University, kmh@ameslab.gov

Prediction of novel stable Fe-V-Si ternary phase

Abstract
Genetic algorithm searches based on a cluster expansion model are performed to search for stable phases of Fe-V-Si ternary. We identify a new thermodynamically, dynamically and mechanically stable ternary phase of Fe5V2Si with 2 formula units in a tetragonal unit cell. The formation energy of this new ternary phase is −36.9 meV/atom below the current ternary convex hull. The magnetic moment of Fe in the new structure varies from −0.30–2.52 μB depending strongly on the number of Fe nearest neighbors. The total magnetic moment is 10.44 μB/unit cell for new Fe5V2Si structure and the system is ordinarily metallic.

Keywords
Intermetallics, Crystal structure prediction, Ternary phase diagram, Magnetism, First-principles calculation

Disciplines
Materials Science and Engineering | Metallurgy

Prediction of novel stable Fe-V-Si ternary phase

Manh Cuong Nguyen[1*], Chong Chen[1], Xin Zhao[1], Jun Liu[1,2], Cai-Zhuang Wang[1] and Kai-Ming Ho[1]

[1]Ames Laboratory, U.S. DOE, and Department of Physics and Astronomy, Iowa State University, Ames, IA 50011, USA

[2]Department of Physics and Astronomy, University of Virginia, Charlottesville, VA 22904, USA

Abstract

Genetic algorithm searches based on a cluster expansion model are performed to search for stable phases of Fe-V-Si ternary. We identify a new thermodynamically, dynamically and mechanically stable ternary phase of Fe_5V_2Si with 2 formula units in a tetragonal unit cell. The formation energy of this new ternary phase is -36.9 meV/atom below the current ternary convex hull. The magnetic moment of Fe in the new structure varies from -0.30 to 2.52 μ_B depending strongly on the number of Fe nearest neighbors. The total magnetic moment is 10.44 μ_B/unit cell for new Fe_5V_2Si structure and the system is ordinarily metallic.

Keywords: Intermetallics, Crystal Structure Prediction, Ternary Phase Diagram, Magnetism, First-Principles Calculation.

* mcnguyen@ameslab.gov

I. Introduction

Finding new stable compounds is always of great interests as the new compounds may offer unique or even exotic physical properties or applications. It is also of great interests in term of finding new physics which does not show in presently existing materials. Theoretically, much effort has been carried out in searching for new materials at both ambient condition[1–9] or in extreme conditions such as high pressure[10–16]. Several global minimization methods have been developed to perform atomic or crystal structure search: Simulated annealing[17], genetic algorithm(GA)[18–20], *ab-initio* random search[21] or particle swarm optimization[22]. For all these methods to work, a fitness evaluator is needed in order to be able to rank the candidates. The most commonly use fitness evaluator is density functional theory (DFT)[23] calculation, which is used to calculate the energy (for ambient condition search) or enthalpy (for high pressure search) of candidate structures. The DFT calculations are heavy and time consuming with computational workload increasing rapidly with system sizes. Most of the theoretical materials predictions have been performed so far are for binary systems. There are predictions for ternary and higher multicomponent alloys as well but they are quite fewer than those for binary alloys. Because there are too many degrees of freedom in crystal structure and in compositional space as well for multicomponent alloys, searches for new stable compounds of multicomponent alloys are very challenging.

Fe-V-Si system has been attracting much attention in both binary and ternary compounds as some of its compounds showing interesting physical phenomena and properties. Heusler alloy Fe_2VSi shows cubic to tetragonal transformation at low temperature[24,25] and an unusual complex structure at high temperature[26]. Heusler-type $Fe_{3-x}V_xSi$ alloys are considered to have relatively high thermoelectric power. They also show some anomalous resistivity properties and a negative Seebeck coefficient at larger value of x[27,28]. Up to date, only one low temperature ternary compound, the Heusler Fe_2VSi, is known for Fe-V-Si system. Some other ternary phases at high temperature were also proposed such as τ_1, τ_2, τ_3 and τ_4 [29]. Among them only τ_4, the high temperature phase of Fe_2VSi, has been clearly solved for the atomic structure[26]. The other 3 phases' atomic structures are unknown and there are very limited information or data about their atomic structures and physical properties. Even the exact chemical compositions of these phases are still under debate. These 3 phases have wide ranges of compositions, e.g., nominal chemical formula of τ_3 is $Fe_5V_3Si_2$ with Fe concentration from 32 to 44 at %. It would be of great interest if more ternary compounds of Fe-V-Si are identified.

In this paper, we use various crystal structure prediction techniques in combination with DFT and cluster expansion method[30,31] to perform an efficient search for stable Fe-rich Fe-V-Si ternary compound. A fast crystal structure search by *ab initio* random search shows that there is a basin of low energy structures with body-centered cubic (BCC) lattice for Fe-rich Fe-V-Si ternary compounds so we can apply constraints on lattice sites during the searches for new stable ternary compounds of Fe-rich Fe-V-Si. Further generic algorithm searches with cluster expansion model identify a new stable ternary compound Fe_5V_2Si. The new Fe_5V_2Si structure is in

ferrimagnetic state with sizable magnetic moment of 0.65 μ_B/atom and very weak magneto-crystalline anisotropy. The new structure is an ordinarily metallic compound.

II. Computational Methods

The spin-polarized density functional theory (DFT)[23] calculations are performed by Vienna *Ab-initio* Simulation Package (VASP)[32] with projector-augmented wave (PAW) pseudo-potential method[33,34] within generalized-gradient approximation (GGA) parameterized by Perdew, Burke, and Ernzerhof (PBE)[35]. The energy cutoff is 300 eV and the Monkhost-Pack scheme[36] is used for Brillouin zone sampling with a high quality k-point grid of $2\pi \times 1/40$ Å^{-1} equivalent to 14 × 14 × 14 k-mesh for BCC Fe structure. For fast screening with the random search method, a lower k-point grid of $2\pi \times 1/25$ Å^{-1} is used. The CE coefficients for BCC Fe-V-Si ternary up to 3rd nearest-neighbor (NN) pair and 2nd NN triplet clusters are fitted by ATAT code[31,37]. Real space cut-and-paste GA [6,7,16,19] are used for crystal structure searches based on the CE model.

III. Results and Discussions

1. Fe-V-Si ternary convex hull

We first construct the Fe-V-Si ternary convex hull based on known phases including pure elements, binary and ternary phases consisting Fe, V and Si. All phases, including the symmetry, lattice parameters and formation energy, are listed in Table I. There are 16 known phases and five of them are high temperature or metastable phases. The high temperature/metastable phases include α-FeSi, β-Fe_2Si, Fe_5Si_3, hT-$FeSi_2$ and V_5Si_3. For a binary, the composition space is just a line so the convex hull is a curve connecting the formation energies of all compositional neighbor stable phases. For a ternary system, the compositional space is a regular triangular piece of a plane as shown in Fig. 3. The convex hull is then comprised of planes connecting the formation energies of all possible 3 stable phases. The surface formed by the bottom pieces of planes at any composition is the convex hull surface. The formation energies of all known stable structures are lying on this convex hull surface. Any new structure having formation energy below this convex hull surface will be new stable structure and the convex hull surface will be constructed again by taking the formation energy of the newly found structure into consideration. From Fig. 3, we can see that the calculated convex hull surface is consistent with experiment. There are 11 stable structures, which are ε-FeSi, Fe_3Si, FeV, V_3Si, c-Fe_2VSi, t-Fe_2VSi, β-$FeSi_2$, β-V_5Si_3, VSi_2, Fe, V and Si respectively. Other 5 structures, shown in red bold font in Table I, are metastable structures in our calculation, which is consistent with experiment.

It is worthwhile to discuss in more details about the only known stable ternary compound Fe_2VSi. This compound exhibits complex and interesting structural properties[24,26]. Fe_2VSi is a Heusler alloy in the $L2_1$ Cu_2MnAl-prototype structure at room temperature[24,25,38]. However, it has a complex α-Mn-based structure at high temperature and the transformation from the simpler

structure at room temperature to a more complex structure at high temperature is a very unusual transformation as pointed out by Nashima *et al*.[26]. At 123K, Fe_2VSi was found to start developing anti-ferromagnetic order and undergoes a structural transformation from high temperature cubic to lower temperature tetragonal structure[24,25]. At 10 K the tetragonal phase has c/a = 0.989[24]. In this work, we are focusing on low energy structures so we do not consider the high temperature α-Mn-based phase of Fe_2VSi. We consider all FM, NM and AFM magnetic phases as well as cubic and tetragonal crystal structure of Fe_2VSi. For AFM in cubic structure, we fully relax structure while keeping the unit cell in cubic during relaxation. Without this constraint, the cubic unit cell will be transformed to a tetragonal unit cell. All other structures are fully relaxed without any constraints.

The FM cubic phase is -15.9 meV/atom more stable than the NM phase and the Fe magnetic moment is $0.49\mu_B$/Fe. This FM phase is also -9.2 meV/atom more stable than the constrained AFM cubic phase. However, FM cubic phase is not the most stable structure. The AFM tetragonal phase is -8.6 meV/atom lower in energy, showing that AFM tetragonal is the ground state structure of Fe_2VSi at low temperature, which is consistent with experiment and previous calculation. The magnetic moment of the Fe in AFM tetragonal phase is 0.84 μ_B/Fe, which is very close to the experiment value of 0.90 μ_B/Fe obtained from neutron scattering[39]. The Fe magnetic moment from our calculation is between experiment and previous calculation (0.83 μ_B/Fe)[40] values. The AFM tetragonal structure from our calculation has c/a = 0.968, which is slightly smaller than the experimentally observed value at 10 K. We would like to note that we also observe from our calculation a second AFM tetragonal phase, namely AFM-2 tetragonal phase, which exhibits magnetic moment of 0.68 μ_B/Fe and has formation energy 3.7 meV/atom higher than that of the AFM tetragonal phase. In contrast with AFM tetragonal phase which has c/a smaller than 1, the AFM-2 tetragonal phase has c/a = 1.067. This can be understood as the cubic to tetragonal transformation having a double wells energy landscape in a quartic functional form. We use the AFM tetragonal phase of Fe_2VSi in our convex hull construction.

2. Low-energy basin of BCC lattice based structures identified by random search

A fast screening for Fe_3VSi, Fe_2V_2Si and Fe_4VSi with 2 and 4 formula units (f.u.) are performed firstly using the random search method. Four hundred structures are randomly generated, with or without crystal symmetry, for each composition and unit cell size. Both the unit cell and atomic coordinates of all structures are then fully relaxed by DFT calculations. Two lowest-energy structures obtained from random searches for each composition are shown in Fig. 2. The corresponding structure symmetry, formation energy and magnetic moment of those structures are shown in Table II. Although these structures have very different unit cells and symmetries, we can see clearly that all these structures have a same BCC underlying lattice. For eye guiding of the underlying BCC lattice, we draw grey squares in each structure to show the BCC unit. The differences between these structures are only on how Fe, V and Si distributed on the BCC lattice sites. We note that not only the lowest-energy structures shown in Fig. 2 have BCC

underlying lattice, all other low-energy structures obtained from random search also belong to BCC lattice. These results imply that there is a favorable basin of BCC lattice based structures for Fe-rich ternary compounds. Therefore, an atomistic structure search scheme focusing on BCC underlying lattice should be more efficient to identify the low energy and ground state structures of Fe-V-Si ternary at the Fe-rich corner of the ternary phase diagram. Cluster expansion (CE) method is basically a machine learning regression model, where the model features are the local environments of a lattice site considering nearby sites at different radius. CE calculation is, therefore, very computationally efficient as the total energy can be calculated as a sum of different interactions, which are fitting parameters. It is also well-known that CE model can calculate the energy of a system very accurately, at the similar level of accuracy used to build the database, which is usually DFT calculation. On the other hand, GA, a population optimization algorithm mimicking the Darwinian evolution in nature, is an efficient global minimization method. Therefore, we can use CE model as an "*auxiliary tool*" to rapidly and efficiently screen candidate structures during the course of structural evolution with GA search. Final best candidate structures will be evaluated again by DFT calculations for better accuracy. In the following, we will further explore structures of Fe-rich Fe-V-Si ternary compounds by combining GA and CE.

3. Cluster expansion model and genetic algorithm search

Cluster expansion coefficients for Fe-V-Si ternary on BCC lattice are fitted based on 65 selected structures from our above mentioned random searches for Fe-rich ternary. We fit the CE model for up to 3rd nearest-neighbor (NN) pairs and 2nd NN triplets by ATAT code[31]. The root mean squared error is 17.0 meV/atom and the cross-validation score, which shows the prediction power of the fitted CE model[31], is 30.0 meV/atom. Fig. 2(a) shows the DFT versus CE energies for the structures used in fitting. We can see a very strong correlation between them and all represent data points fall on or very close to a straight perfect fitting line. Fig. 2(b) shows the values of effective cluster interactions (ECIs) in our CE energy model. The dominant ECI values are from clusters including up to 1st and 2nd NN interactions. The ECI values for cluster including 3rd NN is very small, suggesting that we can truncate the expansion at 3rd NN and inclusion of longer range clusters is not necessary.

We use real space cut-and-paste atomic structure generic algorithm search scheme[6,7,19,41] in our structure search. The total energies of candidate structures are calculated by CE model fitted above. In these GA searches, we use BCC lattice but with difference unit cell sizes and shapes. We search for a wide range of compositions focusing on Fe-rich ternary. Several low-energy structures selected from each composition searches are fully relaxed again by DFT calculations to calculate the energies to determine the stability of the structures against the ternary convex hull.

4. New stable compound

a. Stabilities: Thermodynamics, dynamics and mechanics

We find a new stable ternary compound: Fe_5V_2Si. The crystallographic details of new Fe_5V_2Si structure are given in Table III. It has P4/nmm symmetry (#129) with Z = 2. There are 4 Wyckoff sites for Fe, 2 Wyckoff sites for V and 1 Wyckoff site for Si. The formation energy is –36.9 meV/atom below the convex hull surface constructed based on known structures (blue filled circle on Fig. 3), meaning that the new Fe_5V_2Si is thermodynamically stable again any phase decompositions into other known ternary and binary phases as well as pure elemental phases. When a new convex hull surface is constructed by taking the newly discovered Fe_5V_2Si compound into account, all the previous 11 structures constituting the old convex hull are still on the convex hull surface. So the new convex hull is constructed by previous 11 structures and the new Fe_5V_2Si. These results explain why those 11 structures can be observed experimentally at low temperature. It also indicates that the new Fe_5V_2Si structure should be able to be synthesized in experiment as equilibrium stable structure and it will be the second known ternary compounds at low temperature after Fe_2VSi ternary. We re-verify the stability of Fe_5V_2Si structure against 11 structures constituting the old convex hull within local density approximation (LDA)[42] to make sure that it is indeed a stable phase but not a spurious error of a specific exchange correlation functional. Our LDA calculations show that Fe_5V_2Si structure is -50.8 meV/atom below the convex hull, re-confirming that Fe_5V_2Si is a new true stable structure.

To further investigate the dynamical stability, we perform phonon calculation for the newly found Fe_5V_2Si structure by finite difference method with a 2 x 2 x 2 supercell via Phonopy code[43,44]. The phonon dispersion and density of phonon are shown in Fig. 4. It is clearly that Fe_5V_2Si structure does not possess any imaginary phonon modes, meaning that it is indeed dynamically stable against vibration. We also investigate the mechanical stability of Fe_5V_2Si structure by study moduli and elasticity. The elastic constants (Table IV) are calculated by strain-stress relationship approach[45]. The moduli of tetragonal Fe_5V_2Si are calculated from elastic constants by Voigt-Reuss-Hill approximation[46]. It can be easily verified that elastic constants of Fe_5V_2Si structure satisfy the Born-criteria[47] for mechanical stability, meaning that the Fe_5V_2Si is stable against small distortions. Thus, the newly found Fe_5V_2Si structure is thermodynamically, dynamically and mechanically stable. This finding may draw more research interest in ternary Fe-V-Si and especially we hope that some experimental work would be performed to synthesize the new stable compound. In addition to the new Fe_5V_2Si phase, we also found two other new structures, Fe_4V_2Si and Fe_6V_2Si (shown by triangles on Fig. 3), which are thermodynamically stable with respect to the old convex hull, but become metastable when the new Fe_5V_2Si structure is taken into account. Nevertheless, these two phases would be good metastable phases and would be synthesized under non-equilibrium processing conditions.

b. Electronic and magnetic properties

Figure 5 shows the electronic density of states (DOS) and band structure along high symmetric lines of the Brillouin zone of the newly identified Fe_5V_2Si structure. We can see that Fe_5V_2Si is an ordinarily metallic compound with DOS of 5.8 and 4.2 states/unit cell at Fermi level for spin up and spin down channels, respectively. The Fermi level is close to a minimum of DOS

for both spin up and down components. The Fe_5V_2Si is ferrimagnetic with average magnetic moment of 0.65 μ_B/atom. The magnetic moments at each lattice site are shown in Table III. Si does not exhibit magnetic moment as expected. The magnetic coupling between V and most of Fe (except for Fe on 2*b*-site) is anti-ferromagnetic, which is similar to the magnetic configuration in FeV compound. It is interesting to note that the Fe on 2*b*-site has very small moment and magnetic interaction between this Fe atom and those Fe atoms on other Wyckoff sites is anti-ferromagnetic. From a nearest-neighbor (NN) analysis we find that there is a correlation between the magnitude of magnetic moment of a Fe atom and the number of its NN Fe atoms. Fe on 2*c*-site has 8 Fe atoms as NN, making its local environment similar to that in BCC Fe and subsequently rendering a magnetic moment similar to that of BCC Fe. Fe on 2*a*-site has 4 Fe and 4 V atoms as NN. Fe on 4*f*-site has 2 Fe, 4 V and 2 Si atoms as NN. Fe on 2*b*-site does not have any Fe as NN and its 8 NN are 4 V and 4 Si atoms. This trend of Fe magnetic moment change follows the Slater-Pauling curve if the increase of number of Fe NN is considered the increase of Fe concentration or, in the other words, the increase of number of electron to the system. We also calculated the magneto-crystalline anisotropy energy of Fe_5V_2Si structure. It turned out that the structure has an easy basal plane, the *xy*-plane, and a very small magnetic anisotropy of 9.4 μeV/atom, implying that the newly identified ternary compound is not suitable for permanent magnets. But it can find applications in soft magnets, which do not require a strong favor of an easy axis magnetic anisotropy.

IV. Conclusions

In conclusion, by combining different atomic structure prediction techniques we perform an efficient search for new stable ternary compound of Fe-V-Si system in Fe-rich regime. We find that there is a low energy structure basin consists of structures based on BCC lattice for Fe-rich Fe-V-Si ternary. We identify a new thermodynamically, dynamically and mechanically stable ternary compound Fe_5V_2Si, which has formation energy -36.9 meV/atom lower than the currently known convex hull. The new compound is in ferrimagnetic state with total magnetic moment of 0.65 μ_B/atom and is ordinarily metallic.

Acknowledgements

This work is supported by the U.S. Department of Energy (DOE), Office of Science, Basic Energy Sciences, Materials Science and Engineering Division, including the grant of computer time at the National Energy Research Scientific Computing Center (NERSC) in Berkeley, CA. M. C. N. is also supported by U.S. DOE, Energy Efficiency and Renewable Energy, Vehicles Technology Office, EDT program. The research was performed at Ames Laboratory, which is operated for the U.S. DOE by Iowa State University under contract # DE-AC02-07CH11358.

References

[1] C. He, L. Sun, C. Zhang, X. Peng, K. Zhang, J. Zhong, Four superhard carbon allotropes: a first-principles study, Phys. Chem. Chem. Phys. 14 (2012) 8410. doi:10.1039/c2cp40531h.

[2] Q. Li, Y. Ma, A.R. Oganov, H. Wang, H. Wang, Y. Xu, T. Cui, H.K. Mao, G. Zou, Superhard monoclinic polymorph of carbon, Phys. Rev. Lett. 102 (2009) 175506. doi:10.1103/PhysRevLett.102.175506.

[3] Q. Li, D. Zhou, W. Zheng, Y. Ma, C. Chen, Global structural optimization of tungsten borides, Phys. Rev. Lett. 110 (2013) 130012. doi:10.1103/PhysRevLett.110.136403.

[4] Z. Zhao, B. Xu, X.F. Zhou, L.M. Wang, B. Wen, J. He, Z. Liu, H.T. Wang, Y. Tian, Novel superhard carbon: C-centered orthorhombic C8, Phys. Rev. Lett. 107 (2011) 1–5. doi:10.1103/PhysRevLett.107.215502.

[5] M.C. Nguyen, X. Zhao, M. Ji, C.-Z. Wang, B. Harmon, K.-M. Ho, Atomic structure and magnetic properties of Fe1–xCox alloys, J. Appl. Phys. 111 (2012) 07E338. doi:10.1063/1.3677929.

[6] M.C. Nguyen, J.-H. Choi, X. Zhao, C.-Z. Wang, Z. Zhang, K.-M. Ho, New Layered Structures of Cuprous Chalcogenides as Thin Film Solar Cell Materials: Cu 2 Te and Cu 2 Se, Phys. Rev. Lett. 111 (2013) 165502. doi:10.1103/PhysRevLett.111.165502.

[7] X. Zhao, M.C. Nguyen, W.Y. Zhang, C.Z. Wang, M.J. Kramer, D.J. Sellmyer, X.Z. Li, F. Zhang, L.Q. Ke, V.P. Antropov, K.M. Ho, Exploring the structural complexity of intermetallic compounds by an adaptive genetic algorithm., Phys. Rev. Lett. 112 (2014) 45502. doi:10.1103/PhysRevLett.112.045502.

[8] M.C. Nguyen, X. Zhao, C.-Z. Wang, K.-M. Ho, New Be-intercalated hexagonal boron layer structure of BeB2, RSC Adv. 4 (2014) 15061–15065. doi:10.1039/c4ra00114a.

[9] X. Zhao, M.C. Nguyen, C.-Z. Wang, K.-M. Ho, Structures and stabilities of alkaline earth metal peroxides XO2 (X = Ca, Be, Mg) studied by a genetic algorithm, RSC Adv. 3 (2013) 22135. doi:10.1039/c3ra43617a.

[10] A.R. Oganov, S. Ono, Theoretical and experimental evidence for a post-perovskite phase of MgSiO3 in Earth's D" layer, Nature. 430 (2004) 445–448. doi:10.1038/nature02701.

[11] K. Umemoto, R.M. Wentzcovitch, Prediction of an U2S3-type polymorph of Al2O3 at 3.7 Mbar., Proc. Natl. Acad. Sci. U. S. A. 105 (2008) 6526–30. doi:10.1073/pnas.0711925105.

[12] L. Zhu, Z. Wang, Y. Wang, G. Zou, H. Mao, Y. Ma, Spiral chain O_4 form of dense oxygen., Proc. Natl. Acad. Sci. U. S. A. 109 (2012) 751–3. doi:10.1073/pnas.1119375109.

[13] Y. Wang, H. Liu, J. Lv, L. Zhu, H. Wang, Y. Ma, High pressure partially ionic phase of water ice, Nat. Commun. 2 (2011) 563. http://dx.doi.org/10.1038/ncomms1566.

[14] A.R. Oganov, R.J. Hemley, R.M. Hazen, A.P. Jones, Structure, Bonding, and Mineralogy of Carbon at Extreme Conditions, Rev. Mineral. Geochemistry. 75 (2013) 47–77. doi:10.2138/rmg.2013.75.3.

[15] M. Ji, K. Umemoto, C.-Z. Wang, K.-M. Ho, R.M. Wentzcovitch, Ultrahigh-pressure phases of H2O ice predicted using an adaptive genetic algorithm, Phys. Rev. B. 84 (2011)

220105. doi:10.1103/PhysRevB.84.220105.

[16] S.Q. Wu, M. Ji, C.Z. Wang, M.C. Nguyen, X. Zhao, K. Umemoto, R.M. Wentzcovitch, K.M. Ho, An adaptive genetic algorithm for crystal structure prediction., J. Phys. Condens. Matter. 26 (2014) 35402. doi:10.1088/0953-8984/26/3/035402.

[17] S. Kirkpatrick, C.D. Gelatt Jr., M.P. Vecchi, Optimization by simulated annealing, Science. 220 (1983) 671–680. doi:10.1126/science.220.4598.671.

[18] B. Hartke, Global geometry optimization of clusters using genetic algorithms, J. Phys. Chem. 97 (1993) 9973–9976. doi:10.1021/j100141a013.

[19] D. Deaven, K. Ho, Molecular Geometry Optimization with a Genetic Algorithm, Phys. Rev. Lett. 75 (1995) 288–291. doi:10.1103/PhysRevLett.75.288.

[20] C.W. Glass, A.R. Oganov, N. Hansen, USPEX—Evolutionary crystal structure prediction, Comput. Phys. Commun. 175 (2006) 713–720. doi:10.1016/j.cpc.2006.07.020.

[21] C.J. Pickard, R.J. Needs, High-Pressure Phases of Silane, Phys. Rev. Lett. 97 (2006) 45504. doi:10.1103/PhysRevLett.97.045504.

[22] Y. Wang, J. Lv, L. Zhu, Y. Ma, Crystal structure prediction via particle-swarm optimization, Phys. Rev. B. 82 (2010) 94116. doi:10.1103/PhysRevB.82.094116.

[23] W. Kohn, L.J. Sham, Self-Consistent Equations Including Exchange and Correlation Effects, Phys. Rev. 140 (1965) A1133–A1138. doi:10.1103/PhysRev.140.A1133.

[24] M. Kawakami, S. Nishizaki, T. Fujita, Tetragonal deformation in Fe2VSi at low temperatures, J. Phys. Soc. Japan. 64 (1995) 4081–4083.

[25] K. Endo, H. Matsuda, K. Ooiwa, K. Itoh, Antiferromagnetism in a heusler alloy Fe2VSi, J. Phys. Soc. Japan. 64 (1995) 2329–2332. doi:10.1143/JPSJ.64.2329.

[26] O. Nashima, Y. Yamaguchi, H. Higashi, T. Goto, T. Kaneko, S. Sasamori, H. Kimura, K. Kobayashi, R. Kainuma, K. Ishida, T. Kanomata, Unusual complex high temperature structure of Fe2VSi, J. Alloys Compd. 417 (2006) 150–154. doi:10.1016/j.jallcom.2005.09.046.

[27] O. Nashima, T. Kanomata, Y. Yamaguchi, S. Abe, T. Harada, T. Suzuki, H. Nishihara, K. Koyama, T. Shishido, K. Watanabe, T. Kaneko, Magnetic and electrical properties of Fe3−xVxSi, J. Alloys Compd. 383 (2004) 298–301. doi:10.1016/j.jallcom.2004.04.061.

[28] Y.T. Cui, a. Kimura, K. Miyamoto, K. Sakamoto, T. Xie, S. Qiao, M. Nakatake, K. Shimada, M. Taniguchi, S.-I. Fujimori, Y. Saitoh, K. Kobayashi, T. Kanomata, O. Nashima, Electronic structures of Fe3 -x V x Si probed by photoemission spectroscopy, Phys. Status Solidi. 203 (2006) 2765–2768. doi:10.1002/pssa.200669648.

[29] H. Xu, Y. Du, W. Sun, L. Zhang, Iron – Silicon – Vanadium: Datasheet from Landolt-Börnstein - Group IV Physical Chemistry · Volume 11D5: "Ternary Alloy Systems," (2009). doi:10.1007/978-3-540-70890-2_28.

[30] J.M. Sanchez, F. Ducastelle, D. Gratias, Generalized cluster description of multicomponent systems, Phys. A Stat. Mech. Its Appl. 128 (1984) 334. doi:10.1016/0378-4371(84)90096-7.

[31] A. van de Walle, Multicomponent multisublattice alloys, nonconfigurational entropy and other additions to the Alloy Theoretic Automated Toolkit, Calphad Comput. Coupling Phase Diagrams Thermochem. 33 (2009) 266–278. doi:10.1016/j.calphad.2008.12.005.

[32] G. Kresse, J. Furthmüller, Efficient iterative schemes for ab initio total-energy calculations using a plane-wave basis set, Phys. Rev. B. 54 (1996) 11169. doi:10.1103/PhysRevB.54.11169.

[33] P.E. Blöchl, Projector augmented-wave method, Phys. Rev. B. 50 (1994) 17953. doi:10.1103/PhysRevB.50.17953.

[34] G. Kresse, D. Joubert, From Ultrasoft Pseudopotentials to the Projector Augmented Wave Method, Phys. Rev. B. 59 (1999) 1758–1775. doi:10.1103/PhysRevB.59.1758.

[35] J.P. Perdew, K. Burke, M. Ernzerhof, Generalized Gradient Approximation Made Simple, Phys. Rev. Lett. 77 (1996) 3865–3868. doi:10.1103/PhysRevLett.77.3865.

[36] H.J. Monkhorst, J.D. Pack, Special points for Brillouin-zone integrations, Phys. Rev. B. 13 (1976) 5188–5192. doi:10.1103/PhysRevB.13.5188.

[37] A. van de Walle, G. Ceder, Automating first-principles phase diagram calculations, J. Phase Equilibria. 23 (2002) 348–359. doi:10.1361/105497102770331596.

[38] M. Kawakami, Huge increase in magnetic ordering temperature of Fe2Mn1−xVxSi at intermediate composition, J. Magn. Magn. Mater. 128 (1993) 284–288. doi:10.1016/0304-8853(93)90472-E.

[39] H. Nishihara, K. Ono, K.U. Neumann, K.R.A. Ziebeck, K. Kanomata, NMR of 51V in a Heusler alloy Fe2VSi, J. Alloys Compd. 383 (2004) 302–307. doi:10.1016/j.jallcom.2004.04.029.

[40] S. Fujii, S. Ishida, S. Asano, Antiferromagnetism and atomic disorder in Fe2VSi, J. Phys. Soc. Japan. 73 (2004) 459–463. doi:10.1143/JPSJ.73.459.

[41] M. Ji, C.-Z. Wang, K.-M. Ho, Comparing efficiencies of genetic and minima hopping algorithms for crystal structure prediction., Phys. Chem. Chem. Phys. 12 (2010) 11617–23. doi:10.1039/c004096g.

[42] J.P. Perdew, A. Zunger, Self-interaction correction to density-functional approximations for many-electron systems, Phys. Rev. B. 23 (1981) 5048–5079. doi:10.1103/PhysRevB.23.5048.

[43] K. Parlinski, Z.Q. Li, Y. Kawazoe, First-Principles Determination of the Soft Mode in Cubic ZrO2, Phys. Rev. Lett. 78 (1997) 4063–4066. doi:10.1103/PhysRevLett.78.4063.

[44] A. Togo, F. Oba, I. Tanaka, First-principles calculations of the ferroelastic transition

between rutile-type and CaCl2-type SiO2 at high pressures, Phys. Rev. B. 78 (2008) 134106. doi:10.1103/PhysRevB.78.134106.

[45] Y. Le Page, P. Saxe, Symmetry-general least-squares extraction of elastic data for strained materials from ab initio calculations of stress, Phys. Rev. B. 65 (2002) 104104. doi:10.1103/PhysRevB.65.104104.

[46] R. Hill, The Elastic Behaviour of a Crystalline Aggregate, Proc. Phys. Soc. Sect. A. 65 (1952) 349–354. doi:10.1088/0370-1298/65/5/307.

[47] F. Mouhat, F.X. Coudert, Necessary and sufficient elastic stability conditions in various crystal systems, Phys. Rev. B. 90 (2014) 4–7. doi:10.1103/PhysRevB.90.224104.

Figure Captions

Figure 1. The lowest energy structures from random search for (a) Fe_2V_2Si, (b) Fe_3VSi and (c) Fe_4VSi compounds.

Figure 2. Cluster expansion model for BCC Fe-V-Si: (a) Energy correlation between CE and DFT and (b) the ECI values of the CE model.

Figure 3. Fe-V-Si ternary convex hull based on experimentally known structures. Color shows relative formation energy in meV/atom to the convex hull.

Figure 4. Crystal structure, phonon band structure and density of phonons (DOP) of Fe_5V_2Si. DOP is in arbitrary unit.

Figure 5. DOS and band structure of Fe_5V_2Si. The negative (in blue) and positive (in red) values of DOS are corresponding to spin up and spin down. Left and right band structures are band structures from spin up and spin down, respectively. Fermi level is shifted to zero. Unit of DOS is states/eV/unit cell.

Table Captions

Table I. Structure database of Fe-V-Si system. The formation energy (H) are referenced to Fe, V and Si bulk phases. Phases in bold italic font are metastable phases.

Table II. Symmetry, formation energy (H) and magnetic moment (M) of 2 lowest energy structures from *ab initio* random search for Fe_2V_2Si, Fe_3VSi and Fe_4VSi.

Table III. Crystallographic data of Fe_5V_2Si and magnetic moment of each lattice site.

Table IV. Elastic constants and moduli including bulk (B), Shear (G) and Young (E) in GPa and Poisson ratio (ν) of Fe_5V_2Si structure.

Tables

Phase	Symmetry	a (Å)	b (Å)	c (Å)	H (meV/atom)
α-FeSi	*Pm-3m*	2.756	2.756	2.756	-482.8
ε-FeSi	*$P2_13$*	4.446	4.446	4.446	-507.0
β-Fe_2Si	*P-3m1*	3.924	3.924	4.834	-379.1
Fe_3Si	*Fm-3m*	5.604	5.604	5.604	-322.4
Fe_5Si_3	*$P6_3/mcm$*	6.695	6.695	4.677	-309.2
FeV	*Pm-3m*	2.879	2.879	2.879	-132.5
V_3Si	*Pm-3n*	4.701	4.701	4.701	-459.3
c-Fe_2VSi	*Fm-3m*	5.618	5.618	5.618	-489.4
t-Fe_2VSi	*I4/mmm*	5.691	5.691	5.509	-493.0
β-$FeSi_2$	*Cmce*	9.869	7.766	7.810	-439.6
hT-$FeSi_2$	*P4/mmm*	2.700	2.700	5.143	-381.0
β-V_5Si_3	*I4/mcm*	9.394	9.394	4.728	-583.3
V_5Si_3	*$P6_3/mcm$*	7.114	7.114	4.826	-529.4
VSi_2	*$P6_222$*	4.558	4.558	6.369	-479.3
Fe	*Im-3m*	2.830	2.830	2.830	0.0
V	*Im-3m*	2.995	2.995	2.995	0.0
Si	*Fd-3m*	5.467	5.467	5.467	0.0

Table I. Structure database of Fe-V-Si system. The formation energy (H) are referenced to Fe, V and Si bulk phases. Phases in bold italic font are metastable phases.

Composition		Symmetry	H (meV/atom)	M (μ_B/f.u.)
Fe_2V_2Si	1st	*Amm2*	-431.7	0.31
	2nd	*R-3m*	-428.9	0.00

Fe_3VSi	1st	*I4/m*	-394.7	2.76
	2nd	*Cmcm*	-388.1	3.42
Fe_4VSi	1st	*Cmcm*	-225.8	0.95
	2nd	*Pmma*	-216.9	1.14

Table II. Symmetry, formation energy (H) and magnetic moment (M) of 2 lowest energy structures from *ab initio* random search for Fe_2V_2Si, Fe_3VSi and Fe_4VSi.

Wyckoff site	**Occupation**	***x***	***y***	***z***	**M (μ_B/atom)**
2*a*	Fe	0.75000	0.25000	0.00000	1.71
4*f*	Fe	0.75000	0.25000	0.74573	1.05
2*b*	Fe	0.75000	0.25000	0.50000	-0.30
2*c*	Fe	0.25000	0.25000	0.87536	2.52
2*c*	V	0.25000	0.25000	0.12618	-0.67
2*c*	V	0.25000	0.25000	0.62667	-0.18
2*c*	Si	0.25000	0.25000	0.37697	0.00

Table III. Crystallographic data of Fe_5V_2Si and magnetic moment of each lattice site.

C_{11}	378.8
C_{12}	97.7
C_{13}	202.9
C_{33}	315.7
C_{44}	140.5
C_{66}	73.9
B	230.5
G	99.7
E	261.5
ν	0.31

Table IV. Elastic constants and moduli including bulk (B), Shear (G) and Young (E) in GPa and Poisson ratio (ν) of Fe_5V_2Si structure.

Figures

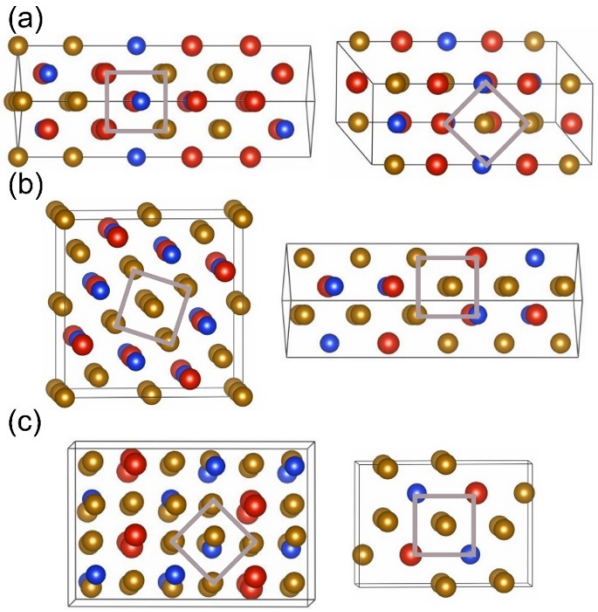

Figure 1. The lowest energy structures from random search for (a) Fe_2V_2Si, (b) Fe_3VSi and (c) Fe_4VSi compounds.

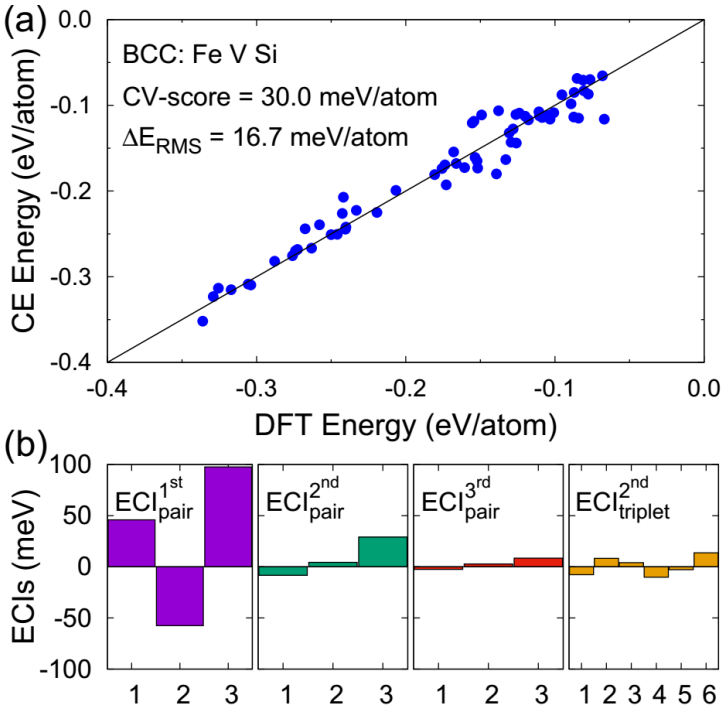

Figure 2. Cluster expansion model for BCC Fe-V-Si: (a) Energy correlation between CE and DFT and (b) the ECI values of the CE model. The *x*-axis stands for different clusters having different chemical decorations.

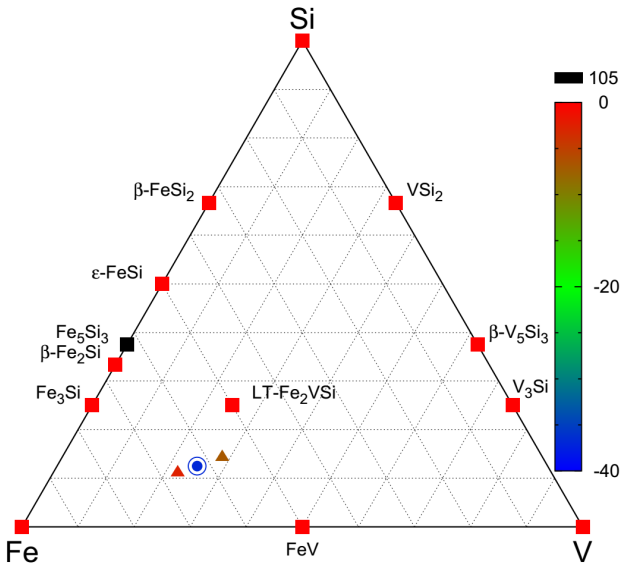

Figure 3. Fe-V-Si ternary convex hull based on experimentally known structures. Color shows relative formation energy in meV/atom to the convex hull.

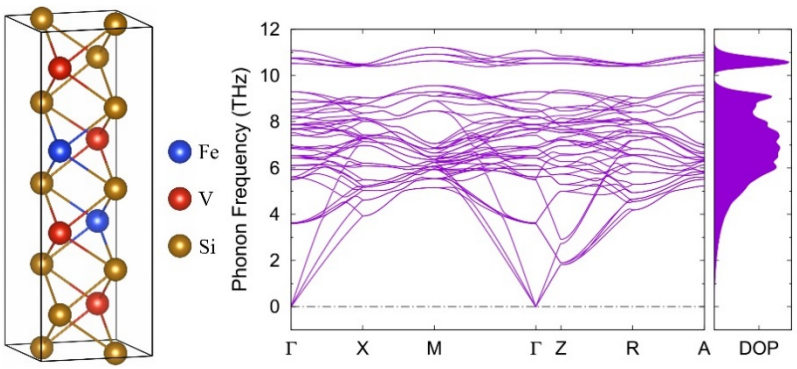

Figure 4. Crystal structure, phonon band structure and density of phonons (DOP) of Fe_5V_2Si. DOP is in arbitrary unit.

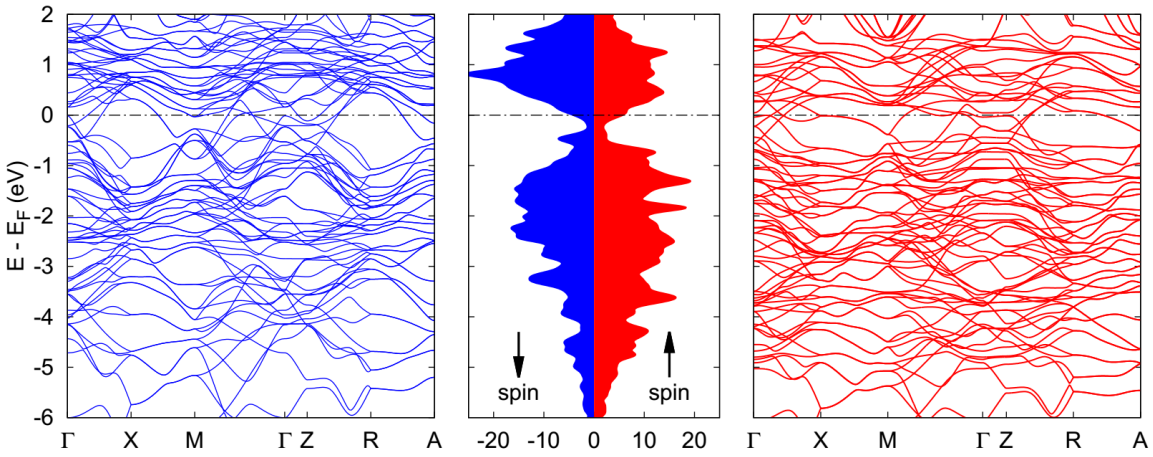

Figure 5. DOS and band structure of Fe_5V_2Si. The negative (in blue) and positive (in red) values of DOS are corresponding to spin up and spin down. Left and right band structures are band structures from spin up and spin down, respectively. Fermi level is shifted to zero. Unit of DOS is states/eV/unit cell.